



Estimation the Efficiency of Sunlight UV on Inactivation COVID-19 Virus

Wisam Kadhum H. Alhashemi^{1*}, Dheaa Sh. Zageer², Hussam K. Risan³

¹ College of Science, Al-Nahrain University, Baghdad, Iraq

² Forensic DNA Center and College of Science, Al-Nahrain University, Baghdad, Iraq

³ College of Engineering, Al-Nahrain University, Baghdad, Iraq



CrossMark

Abstract

The UV radiation of sunlight is considered the main source of microbial germicide and environmental sterilization. The objective of this study includes the estimation of the UV dose amount and time, which required to inactivate coronaviruses by solar exposure. The mean with its confident interval of the unified D90-254 nm inactivation dose (ultraviolet dose for 90% inactivation at 254nm) in several trials published on coronaviruses families, was assumed as ultraviolet susceptibility of the SARS-CoV-2 (COVID-19) virus. The inactivation dose spectrum (sensitivity envelope) for coronaviruses as a function of the UV wavelength equivalent to UVB range (280 to 320 nm) was adopted from literature. The UVB solar measurement intensity at Baghdad's geographical location was used over a year at every fifteen minutes and converted from a lump sum to solar spectrum per wavelength in the range of 280 to 320 nm using a simplified mathematical model. A composite action spectrum was drawn that including the virus sensitivity spectrum normalized to 254 nm, UVB solar measurements spectrum, and inactivation effective dose spectrum for coronaviruses. The area under the inactivation effective dose spectrum was calculated numerically to find the equivalent solar flux. The time required to inactivation the SARS-CoV-2 (COVID-19) virus is predicted for each value of UVB lump sum intensity to simulate the time required to sterility the outdoor surfaces at all months within Baghdad geographical station. the time required for sterilization ranged from 92.9 minutes at solar flux 0.56 J/m²254/min in July, to 371.4 minutes at solar flux 0.14 J/m²254/min in January for the year of data used. This work would be useful to provide the decision-makers with a clear picture of the sterilization process management of the outdoor surfaces and curfew timing arrangement.

Keywords: UV-Index; UVA; UVB; Corona Viruses; Sunlight UV dose, Outdoor surfaces; UV dose time; UV reading stations; COVID-19 Virus.

Introduction

Ultraviolet (UV) ray is part of the electromagnetic solar spectra, where part of the energy is emitted by the sun in the form of electromagnetic waves with various wavelengths and associated energies. The Ultraviolet UV rays are a form of electromagnetic radiation with a wavelength from 10 to 400 nm. The Normal Oxygen O₂ is absorbed most of the electromagnetic waves in the wavelength region of 120 nm to 220 nm. In the wavelength region of range from 50 nm to 120 nm, both the normal Oxygen O₂ and Nitrogen N₂ are cooperating in approximate identical share in observing these waves. Either Ozone or triple Oxygen O₃ is responsible to absorb the waves of the nanometer range from (220-320) of the ultraviolet region[1]. Usually, the ultraviolet UV region is divided according to their wavelength nanometer into three types named UVC, UVB, and

UVA as in Fig.1. The UVC is characterized by a wavelength of 100-280 nm. This range of UV is extremely dangerous to life in all various forms. Fortunately, the Ozone layer absorbs this kind of wave completely before reaching the surface of the earth. In the UVB, the wavelength of this kind of wave ranges between 280-320 nm. The effect of ozone as absorbent on this section varies according to its wavelength as it is considered as an effective absorbent to the shorter wavelengths near 280 and slightly above but weakly absorbent in longer wavelength. Hence, a portion of UVB reaches the surface of the earth. This type of wave affects plants, animals, microbes, as well as the human being. For humans, it causes redness of the skin and eye inflammation and may be activated Skin cancer, eye ulcers, and weaken the body's immune system for prolonged exposure. For microbes, it causes inactivation and may be used as biodefense if sufficient dose and time of exposure are satisfied. In the final kind of UVA, the wavelengths range between

*Corresponding author e-mail: wisamchem1@yahoo.com; (Wisam Kadhum H. Alhashemi).

Receive Date: 18 August 2020, Revise Date: 06 March 2021, Accept Date: 24 March 2021

DOI: 10.21608/EJCHEM.2021.39728.2810

©2021 National Information and Documentation Center (NIDOC)

320-400 nm. In this type, the Ozone is only responsible to absorb ridiculously small quantities. A human being needs this type of radiation to provide them with vitamin D. But still for a long exposure to this type leads to dangerous effects on human life and multiple diseases. This part of waves also slightly makes the microbes lose their life providing adequate exposure. So, the UV radiation of the sunlight may be a bane or a boon[2]-[3][4][5].

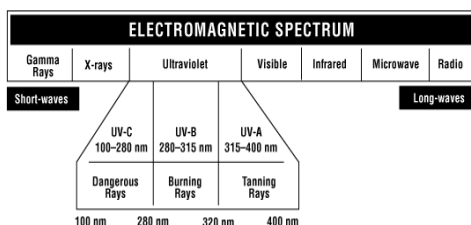


Fig.1 Electromagnetic spectrum [3]

In biological war, there is a predominated thumb rule that stated the bacteria is considered a potential threat source as compared to viruses. This thumb rule is based on the concept that bacteria can withstand environmental conditions longer time than viruses. From an epidemiology point of view, the hardens of viral agents and velocity of spread is not taken into account as what happened in the Covid-19 virus (SARS-CoV-2) in 2020 due to the fast ability to spread and easy transfer from an infected person to a healthy one.

It is known that ultraviolet (UV) works as a virucide inactivation tool available in nature due to damaging their nucleic acids. The UVC range of ultraviolet rays in specifically 260 nm is considered the strongest wavelength for killing. But this range is disappearing in the ozone layer. So, based on the sunlight that reached the ground level, the UVB and UVA ranges of the solar spectrum can take the role of the UVC portion for inactivation purposes on the ground surfaces. UVB and UVA can kill the microbes but with lower efficiency compared with UVC [6]-[7]-[8]-[9]. To find the efficiency of sunlight solar in killing microbes, it is required to calculate the UV viruses' sensitivity in terms of UVB and UVA ranges and to record the sunlight solar UV at the geographic point under consideration. Unfortunately, most of the literature information related to UV viruses' inactivation was used artificial UVC type of radiation at a specific wavelength of 254 nm which is not included in the sunlight radiation that reaches the ground surface of the earth. The sunlight radiation is started from 280 nm to 400 nm[9]. On another side, the good news is based on photochemical science that stated the viruses germicidal occur at all wavelengths within sunlight solar radiation but with varying efficiency depending on the wavelength values[6]. Viruses' inactivation

action spectrum must be constructed based on extrapolation from UV254 data to draw the sensitivity envelop for most viruses by using so-called wavelength dependence. The virus's genome is considered completely responsible for the absorption of UV radiation. While the other virus's constituents play minor roles in the absorption process [6]. Most viruses including the corona family have free nucleic acids with the same order of UV254 sensitivities magnitudes[10]-[11]-[12]-[13]-[14].

The ultraviolet UV of sunlight placed on the earth's surface depends primarily on the direct sunbeam that strength is depending basically on the solar zenith angle. The solar zenith angle (SZA) is defined as the angle measured between the perpendicular vertical line - drawn from the earth at the point under consideration and the line passes from this point to the sun [7]. Also, the sunlight solar ultraviolet UV reached to the earth's surface depends secondary on the weather and sky conditions[15]. The zenith angle (SZA) is a function with time along a day and its value becomes minimum at noon[9]. So, it is expected that the radiation strength is maximum at noon and decreases approximately in the symmetrical distribution before and afternoon. Unfortunately, the solar irradiance records used in predicting virucidal efficiency at Baghdad or in general Iraq are not available per specific wavelengths. The only international recording data are available as shown in the internet free online website of TEMIS satellite ozone data at Baghdad station only[16]. It has longitudinal and latitudinal 44.43 and 33.30 respectively. The data were recorded at noon only based on cloud-free and cloud-modified in terms of erythral UV index and UV dose. The recorded history was from 01/07/2002 up to date. These data need to be transformed and calibrated using an appropriate mathematical model in terms of solar irradiance as a function of the desired veridical wavelength. Complementary information can be obtained for the standard erythral UV weighted fractional spectrum (erythral UV sensitivity curve or envelope). To generalize the procedure from the Baghdad station at noon to all time zone and all Iraq country the website by Meteored <https://www.meteored.com.ve/mapas-meteorologicos/uvi-vencol.html> is used for this purpose. This website is drawn the Iraq UV-Index map for every week based on eight readings of each day as an example in Fig.2.



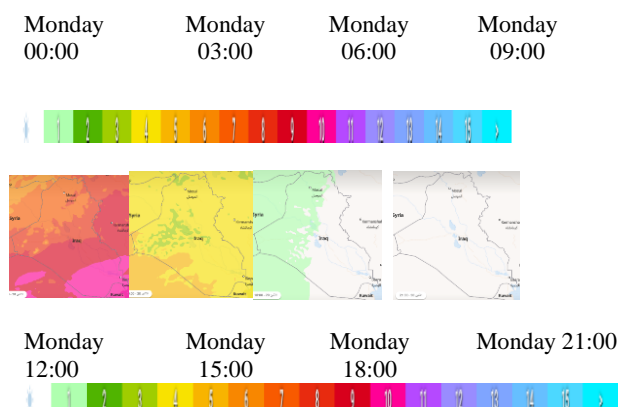


Fig.2: UV-Index in Iraq on 20 April 2020

Fortunately, there are one (In fact, it is the only one) local recording data are available based on solar system recording device (Solar radiation station and an automatic weather station named DAVIS VANTAGE PRO2) located at Atmospheric Science Data Center, College of science, Mustansiriyah University, Baghdad Iraq as shown in Fig.3 (33°08'44"N, 44°05'53" E, altitude 56 m). The data were recorded at this location only and it can be used for Baghdad Governorate. These data are described as the lump sum of the UVB Radiation (280 to 320 nm) which is recording every fifteen minutes. The recorded history was from 09/09/2014 up to date. These data need to be transformed from UVB as a lump sum (W/m^2) to UVB as a spectrum which is a function of the wavelength (W/m^2 per nm) for the wavelength range from 280 to 320 nm. This mathematical transformation was done using an appropriate mathematical model. The last model is used in this study.

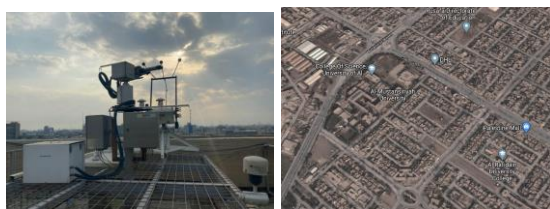


Fig.3: Solar radiation station system at Al-Mustansiriyah University, Baghdad.

A novel corona virus-2019 (severe acute respiratory syndrome coronavirus-2 (SARS-CoV-2) or Covid-19 virus) is one of the members of genus beta-coronaviruses and subgenus Sarbecoronavirus which include severe acute respiratory syndrome-related coronavirus (SARS-CoV) and the Middle East respiratory syndrome (MERS-CoV). They all species of coronaviruses which constitute the subfamily named Orthocoronavirinae under the family titled Coronaviridae which is under order Nidovirales and high-level realm Riboviria[17]-[18]. It is known that coronaviruses species are large Pleomorphous

spherical particles with globular surface projections. The mean diameter of the virus particles is approximately 120 nm (0.12 μm). The diameter of the envelope is ~ 80 nm (0.08 μm) and the spikes are ~ 20 nm (0.02 μm) long. The envelope of the virus under electron micrographs appears as a definite pair of electron-dense shells [19]-[20]. The coronavirus's basic components are shown in Fig.4. It is an enveloped positive-sense single-stranded RNA virus that enters its host cell by binding to the angiotensin-converting enzyme 2 (ACE2) receptor[21]. SARS-CoV-2 was first identified in hospitalized patients in Wuhan, China, in December 2019 and January 2020. It has sequence identity in conserved replicase domains less than 90% between the Covid-19 virus and other members of beta-coronavirus[22]. The major differences within the Nidovirus families are in the number, type, and size of the structural proteins. These differences cause significant alterations in the structure and morphology of the nucleocapsids and virions. It's one of the very largest genomes for RNA viruses, ranged (26-33 kilobases)[23]-[24]-[25]. Several studies stated the susceptibility of coronavirus to ultraviolet radiation[26]-[27]-[28]-[29]. UV irradiation is a widely used method for disinfection against microorganisms including viruses. UV irradiation damages the viruses' genomic materials through changes in their nucleic acids. This phenomenon resulted from the photochemical combination of two adjacent pyrimidines into covalently linked converting it to dimers- photodimerization process. Also, UV radiation results in protein denaturation. As a result of huge damage in these materials especially in the germicidal UV region between 200-300 nm, inactivation of these microorganisms will be the last event in this process[30]-[31].

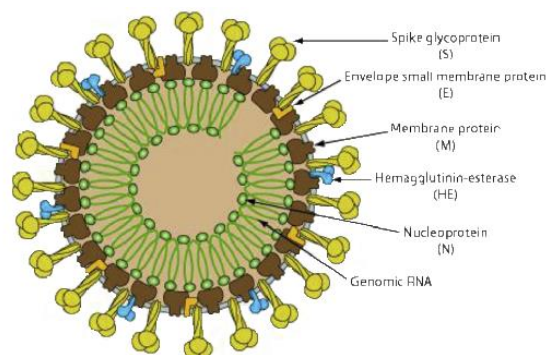


Fig.4: Coronavirus schematic diagram*
 *(<http://ruleofsix.fieldofscience.com/2012/09/a-new-coronavirus-should-youcare.html>)

The objective of the present paper is to use a suitable procedure to scale the UV254 germicidal radiation as

a weighted fractional spectrum (UV sensitivity curve or envelope) based on different genome sizes and equivalent to UVB spectrum wavelength. This envelope is used to estimate the sensitivities to UV254 within the range of ultraviolet sunlight radiation on the ground surface. Corona virus's family is the main part of the scope of this target. Also, in the present study an attempt to develop a method to convert UVB radiation as a lump sum which is the available data in Baghdad to equivalent ultraviolet UVB virucidal spectrum as per wavelength. The overall goal of this study is to evaluate the efficiency of the sunlight UV at Baghdad ground surface in terms of corona virus's family inactivation. The inactivation using environmental nature sunlight is providing the decision-makers to the outdoor surface sterilization process and accordingly arrange the curfew timing. In general, the inactivation is considered as a baseline to estimate for the contaminated areas the recovery time required after a biological attack.

Method

UV Exposure Dose (Fluence): When viruses are exposed to UV irradiation then they are subjected to an exposure dose which is named fluence. The exposure dose (fluence), D (J/m^2) is defined as a function of the irradiance, IR (W/m^2) multiplied by the exposure time, ET as below:

$$D = ET \times IR \quad (1)$$

When the UV dose give, for example in a 37% disinfection rate (63% survival), it is referred to as a D_{37} . While when the UV dose give, for example in a 90% disinfection rate (10% survival), it is referred to as a D_{90} . The D_{90} value is frequently used as an indicator of system size and can be used to assess the survival rate of individual microbes.

The classical exponential decay model is considered as the primary model used to evaluate the survival of microorganisms subject to UV exposure. This model is named a first-order decay rate model. If by providing that, the UV dose is within first-order parameters, then this model is assumed to be adequate for most ultraviolet germicidal inactivation (UVGI) design purposes.

The reason for that is approximately 90 to 99 % of disinfection rates can be achieved in the first stage of decay (Fig.5a). This model can be expressed as[32]:

$$S = e^{-kD} \quad (2)$$

Where D is the dose required, S is the survival fraction, and k is the UV rate constant m^2/J . It is known that a tiny fraction of the microbial population shows a higher level of resistance in general disinfection and especially in UV disinfection [33]. The surviving population is often an order of magnitude more

resistant to UV, When the exposure dose is sufficient to provoke several logs of reduction (i.e. 99% disinfection or higher) in the microbial population. This means that the resistant population as UV rate constant is ten times less compared to the first stage. So, the microbial population's behavior can be assumed to consist of two populations. The first one is named relatively susceptible or fast decay (first stage of decay) that defined by the susceptible portion of the population. While the other population is titled as relatively resistant or slow decay (second stage of decay) will be defined by the resistant population. A famous model for two stage decay has been derived early[34]. In this model 'f' is defined as the resistant fraction and $(1-f)$ is defined as the fast decay fraction as a complement. Further in this model, the constant k_1 represents the first stage (fast decay) rate constant while k_2 is represents the second stage (slow decay) rate constant (Fig.5b). The two populations' survival can be expressed simply by the sum of each decay rate calculated per each contribution, as follows.

$$S = (1 - f)e^{-k_1D} + fe^{-k_2D} \quad (3)$$



(a): First stage decay

(b): Second stage decay

Fig.5: Survival of microbe under UV irradiance [14].

The measured UV254 sensitivities for RNA-containing coronaviruses of several trials whose hosts are vertebrates under ultraviolet light exposure UV254 with different species are shown in Table 1. The D_{50} value that indicates the ultraviolet dose for 50% inactivation is converted according to Eq.2 to the equivalent D_{90} value which indicates only 10% survival. The viruses with only genome size information are known, the D_{90} value is predicted according to interpolation based on other viruses that both D_{90} and genome size are known. The standard deviation of UV254- D_{90} values is 44.9 J/m^2 while the range is between 3-120 J/m^2 . Despite a wide range of variation in the D_{90} values, the mean value of 51.9 J/m^2 with a mean standard error of 14.2 J/m^2 and 95% confidence interval ranged between 19.8 to 84.0 J/m^2 should properly represent the ultraviolet susceptibility of the SARS-CoV-2 (COVID-19) virus. The test of normality of the D_{90} values is carried out as in Fig.6a that indicates the distribution of D_{90} values is subject

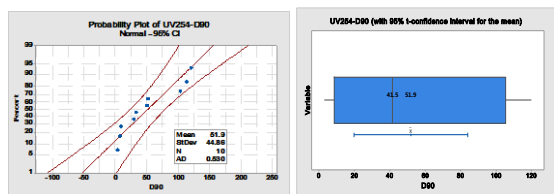
to a normal distribution with an amount of deviation. This behavior of D90 values are appeared also in the boxplot shown in Fig.6b with acceptable symmetry without outliers' observation.

Table 1: Measured, calculated and predicted UV₂₅₄ sensitivities for Coronaviruses

Virus name	D ₉₀ (J/m ²)	D ₉₀ (J/m ²)	Media	Genome size (base pairs kb)	R ef.
Berne virus (Coronaviridae)	7	-	Water	28.475	[3 5]
Coronavirus (MHV)	3	-	Air	30.738	[2 6]
Coronavirus (SARS)	9	-	Water	29.751	[3 6]
Coronavirus (SARS)	11	-	Water	29.751	[3 7]
SARS Coronavirus	12	-	Water	29.751	[2 9]
Murine Coronavirus (MHV)	29	-	Virus suspension	31.335	[3 8]
Murine Coronavirus (MHV)	10	-	Water	31.335	[3 9]
MERS Coronavirus	50 C*	15	Blood, Platelet concentrated	30.108	[4 0]
SARS Coronavirus	33 C*	10	Blood, Platelet concentrated	29.751	[4 1]
SARS-CoV-2	-	-	-	29.844	[4 2]
SARS-CoV-2	-	-	-	29.891	[4 3]
SARS-CoV-2	52 P*	-	-	29.811	[4 4]
SARS-CoV-2	-	-	-	29.903	[4 5]
Statistics	Mean 51.9	St. Dev. 44.9	SE Mean 14.2	95% CI (19.8; 84.0)	

*The letter (C)Used for the calculated D₉₀ according to Eq.2.

**The letter (P)used for the predicted D₉₀ according to genome size interpolation with equivalent viruses of known D₉₀ and genome size.



(a) Normal Plot (b) Box Plot

Fig.6: Normal and Box plots for UV₂₅₄-D₉₀

Virus inactivation spectrum: The previously published action spectra that draw the virus inactivation were analyzed and compiled by David et al [24]. Because these data were combining based on ultraviolet at 254 nm (UV254), so all other wavelengths data were normalized to equivalent 254 nm UV. This was done by calculating the relative sensitivity that was defined as a ratio of any desired wavelength under interest to the specific 254 nm wavelength. For more illustration, if 0.5 relative sensitivity is assumed, then it indicates that the interesting wavelength is just half as effective for virus inactivation as UV254 at the same J/m² exposure level. UV wavelengths above 280 nm are only analyzed due to their availability from the solar radiation that reached the ground surface. It is proved also that there was a little difference between actions

spectra calculated for different viruses' families from the mean values for the different types of nucleic acids. Fig.7 represents the constructed curve from the previous pooled data that showing the relative UV sensitivity (normalized to 254 nm) along the wavelength range required for this study. Fig.6 of sensitivity spectrum can be used for any value of percent of virus survival.

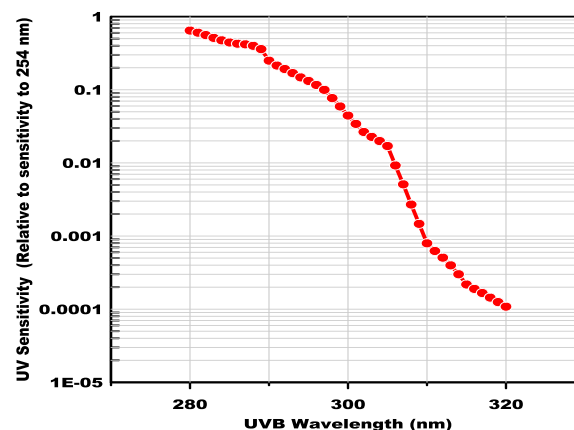


Fig.7: UVB action spectrum for virus inactivation that normalized to 254 nm [24].

Results and discussions

Fig.8 was produced depending on The data available by solar radiation station and an automatic weather station named DAVIS VANTAGE PRO2 which is placed at Atmospheric Science Data Center, College of science, Mustansiriyah University. It shows a solar spectrum UVB radiation as a lump sum in W/m² as a record at Baghdad for a full typical year in 2015 for every fifteen minutes. The value of the maximum averaged level of a lump sum UVB is ranged from 1.6 W/m² at the hottest months (approximately in July and August) to 0.4 W/m² at the coldest months (about at January and February). For more clarity, Fig.9 produced. it describing a solar spectrum UVB radiation as a lump sum in W/m² for two consecutive months (August and September) in the same year of Fig.8. From this figure (Fig. 8), it is observed that the maximum average level for the UVB in August and September are 1.4 and 0.8, respectively. The UVB radiation W/m² record for one day in August 2015 is shown in Fig.10. The variation of the UVB values along the day is subjected to a normal distribution with a maximum at noon and reduced symmetrically from two sides.

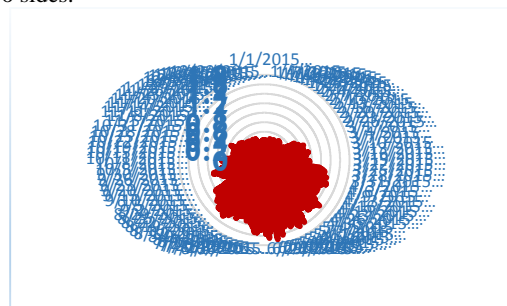
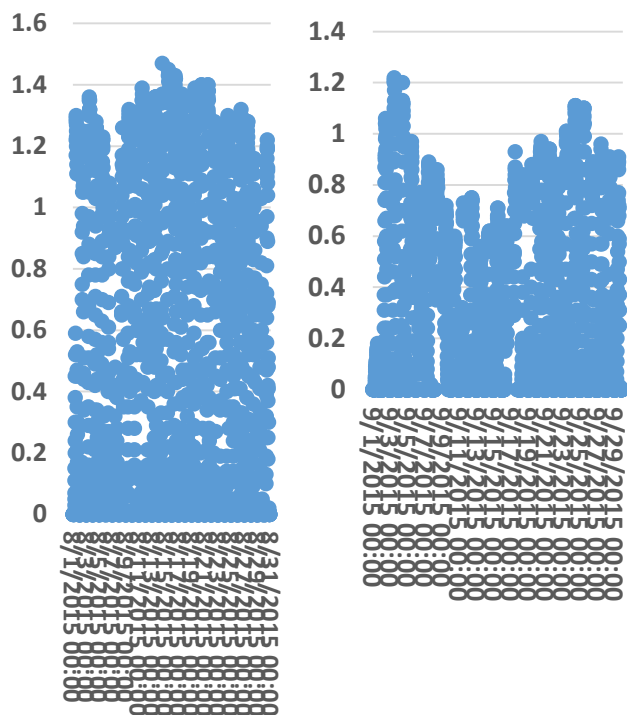


Fig.8: UVB radiation W/m² record at Baghdad for full 2015 year

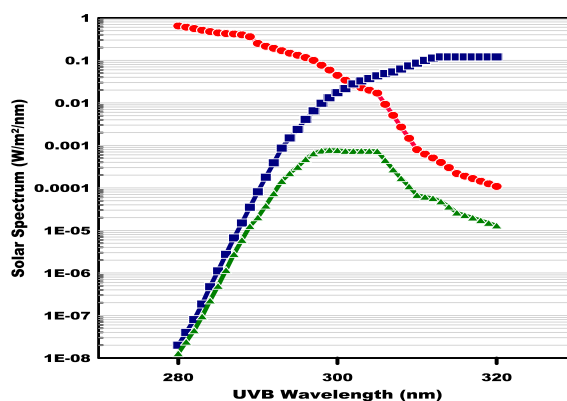
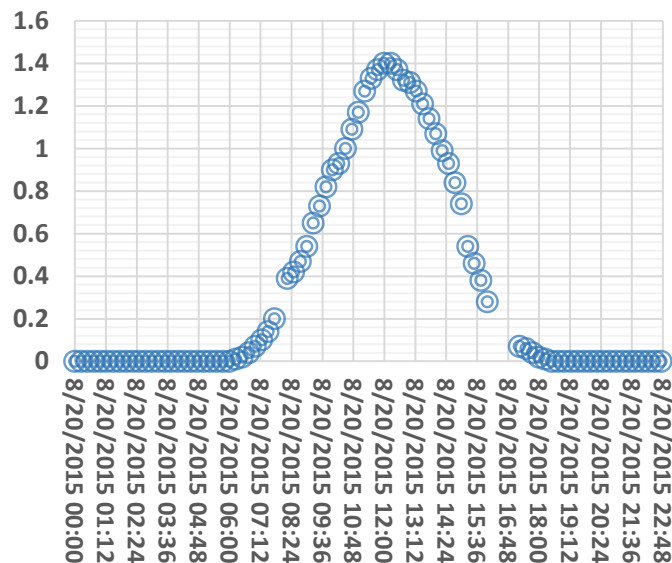
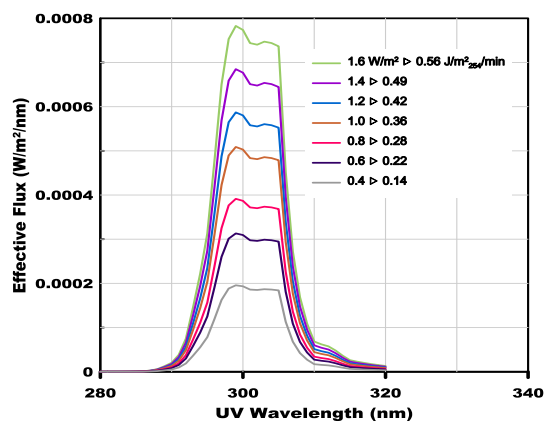


(A): UVB August Record

(B): UVB September Record

Fig.9: UVB radiation W/m^2 record at Baghdad for two months in 2015

Fig.7 as mentioned before represented the relative UV sensitivity (normalized to 254 nm) for the wavelength from 280 to 320 nm that required for this analysis. In other words, all data of UV sensitivity in wavelengths between 280 to 320 nm manipulate to become as in 254 nm. The composite action spectrum was drawn in Fig.11. The overall spectrum includes the virus sensitivity to 254 nm spectrum (the same envelope of Fig.1) and the solar UVB spectrum at a maximum level of $1.6 W/m^2$ after transformation the lump sum measured solar UVB in W/m^2 to solar UVB spectrum in $W/m^2/nm$ using simplified mathematical parabolic assumption with the equivalent area. Fig.11 also includes the effective solar virus inactivation flux spectrum calculated by multiplying the 254 nm normalized sensitivity spectrum times the solar measured transformed spectrum at each wavelength. The effective solar virus inactivation flux spectrum result from this multiplication was numerically integrated by trapezoidal rule with a constant wavelength step of 1 nm to obtain 254 nm equivalent virus inactivation equivalent flux in W/m^2_{254} . The effective solar flux spectrum at different lump sum of UVB (1.6, 1.4, 1.2, 1.0, 0.8, 0.4 W/m^2) is presented on linear scale in Fig.12 with values ranged from (0.56, 0.49, 0.42, 0.36, 0.28, 0.22, 0.14 $J/m^2_{254}/min$) respectively.

Fig.10: UVB radiation W/m^2 record at Baghdad for one day in August 2015.Fig.11: Composite action spectrum consists of virus sensitivity normalized to 245 nm (red line with circles) (Fig.7), UVB solar spectrum as a lump sum of $1.6 W/m^2$ (Blue line with squares), and virus inactivation effective spectrum (Green line with triangles).Fig.12: Virus inactivation effective spectrum at different lump sum UVB W/m^2 .

To find out how the virucidal effect of solar UV compared from one time to another, data from the Atmospheric Science Data Center were used to calculate effective solar fluxes for Baghdad geographical locations at selected times of the year as shown in Table 2. The data were selected for a typical full year with one reading every fifteen minutes. The shape of the flux curve over the day showed the typical symmetrical bell shape. The data in Table 2 demonstrate a general correlation between the equivalent solar flux or intensity (J/m^2 254/min) and UV254 Exposure dose D_{90} [J/m^2]. The equivalent solar flux was calculated for different values (0.56, 0.49, 0.42, 0.36, 0.28, 0.22, 0.14 $J/m^2_{254}/min$) to represent the variation along the months at a typical year. So, Table 2 are assessment times for virus inactivation by solar exposure for each date of a typical year a Baghdad geographical location as represented for various UVB solar radiation with maximum value levels (1.6, 1.4, 1.2, 1.0, 0.8, 0.4 W/m^2). The estimated inactivation time is based on the selected UV₂₅₄ sensitivity D_{90} for coronavirus as a potential interest in biodefense in this study that

ranged from 3 to 129 J/m^2 . Also, the inactivation time is calculated based on the sample mean of UVB₂₅₄- D_{90} , and in its 95% confident interval. The results in term of inactivation time required to indicate that some months along the year, the virus could be inactivated by solar radiation rather quickly, while in other months could persist for a long time. The month is calibrated in terms of equivalent solar flux ($J/m^2_{254}/min$) which is based on a measured solar UVB lump sum (W/m^2). It's very clear from the result stated in table 2 that time required for inactivation in summer months (that have more UVB₂₅₄Exposure) is much less than in winter's months (which have less UVB₂₅₄Exposure). These results were agreed with Jay Herman et al.[46] . the data for Baghdad city produced in table 2 in the hottest summer months for the time required, for inactivation, ranged from 35.3 to 150 min. and from 370.4 to 600 in winter. This result is close to the results of J.I.Sagripanti & C.D.Lytle study - that deduced the time for several cities in the world including Baghdad- which stated in summer 18 min. and in winter 300 min. [47]

Table 2: Virus Inactivation time required in minutes.

Virus name	UVB ₂₅₄ Exposure $D_{90}[J/m^2]$	Equivalent solar flux ($J/m^2_{254}/min$)						
		0.56	0.49	0.42	0.36	0.28	0.22	0.14
Berne virus (Coronaviridae)	7	12.5	14.3	16.7	19.4	25.0	31.8	50.0
Coronavirus (MHV)	3	5.4	6.1	7.1	8.3	10.7	13.6	21.4
Coronavirus (SARS)	9	16.1	18.4	21.4	25.0	32.1	40.9	64.3
Coronavirus (SARS)	113	201.8	230.6	269.0	313.9	403.6	513.6	807.1
SARS Coronavirus	120	214.3	244.9	285.7	333.3	428.6	545.6	857.1
Murine Coronavirus (MHV)	29	51.8	59.2	69.0	80.6	103.6	131.8	207.1
Murine Coronavirus (MHV)	103	184.0	210.2	245.2	286.1	367.9	468.2	735.8
MERS Coronavirus	50	89.3	102.0	119.0	138.9	178.6	227.3	357.1
SARS Coronavirus	33	58.9	67.3	78.6	78.6	117.9	150.0	235.7
SARS-CoV-2	52	92.9	106.1	123.8	422.2	185.7	236.4	371.4
Lower Confident Level	19.8	35.3	40.4	47.1	55.0	70.7	90.0	141.4
Sample Mean	51.9	92.7	105.9	123.6	144.2	185.4	235.9	370.7
Upper Confident Level	84.0	150.0	171.4	200.0	233.3	300.0	381.8	600.0

Note: data in black represent virus Inactivation time required in minutes.

Conclusion

In a conclusion, the estimated time required to inactivate the SARS-CoV-2 (COVID-19) virus at Baghdad geographical location for the outdoor surfaces under solar radiation for all months of the year considered a useful tool to plan the required countermeasures. Hence this study is concerned with coronaviruses in Baghdad geographical location, this study approach can be adopted to predict any virus survival after its release at any place and time of a year when the experimental specific data for any virus inactivation under consideration lacks.

Acknowledgment

This work was supported by Atmospheric Science Data Center, College of science, Mustansiriyah University, Baghdad Iraq in providing the authors with

the solar UVB data for Baghdad geographical location.

References

- [1] G. Megie, "Laser Remote Sensing: Fundamentals and Applications," *Eos, Trans. Am. Geophys. Union*, vol. 66, no. 40, p. 686, Oct. 1985, DOI: 10.1029/EO066i040p00686-05.
- [2] F. K. Lutgens and E. J. Tarbuck, "The atmosphere: An introduction to meteorology eleventh edition." Prentice Hall, New York, 508 pp, 2010.
- [3] Y. J. Kim *et al.*, "Complete genome sequence of Middle East respiratory syndrome coronavirus KOR/KNIH/002_05_2015, isolated in South Korea," *Genome Announc.*, vol. 3, no. 4, pp. 5–6, 2015, doi:

- 10.1128/genomeA.00787-15.
- [4] S. M. M. Abd EL-Aziz, A. M. E. Abd EL-Salam, M. S. Salama, and D. M. Mahmoud, "Effect of Ultraviolet Radiation on Original Activity Remaining of *Spodoptera littoralis* NPV against *S. Littoralis* Boisd (Lepidoptera: Noctuidae)," *Egypt. J. Chem.*, vol. 62, pp. 173–178, 2019, doi: 10.21608/EJCHEM.2019.12680.1786.
- [5] M. Kamal, E. Mahmoud, A. Hassabo, and M. Eid, "Effect of Some Construction Factors of Bi-layer Knitted Fabrics Produced for Sports Wear on Resisting Ultraviolet Radiation," *Egypt. J. Chem.*, vol. 0, no. 0, pp. 0–0, 2020, doi: 10.21608/ejchem.2020.25922.2514.
- [6] A. M. Rauth, "The Physical State of Viral Nucleic Acid and the Sensitivity of Viruses to Ultraviolet Light," *Biophys. J.*, vol. 5, no. 3, pp. 257–273, 1965, doi: [https://doi.org/10.1016/S0006-3495\(65\)86715-7](https://doi.org/10.1016/S0006-3495(65)86715-7).
- [7] J. A. Parrish, R. H. Anderson, F. Urbach, and D. Pitts, "UVA-biological Effects of Ultraviolet Radiation with Emphasis on Human Responses to Long-wave Ultraviolet, f.³filenum Press," *New York*, 1978.
- [8] R. Setlow, "The use of action spectra to determine the physical state of DNA in vivo.," *Biochim. Biophys. Acta*, vol. 39, p. 180, 1960.
- [9] J. H. Gibson, "UVB radiation: definition and characteristics," *USDA/CSU website.[Online.] http://uvb. nrel. colostate. edu*, 2003.
- [10] K. Furuse and I. Watanabe, "Effects of ultraviolet light (UV) irradiation on RNA phage in H₂O and in D₂O.," *Virology*, vol. 46, no. 1, p. 171, 1971.
- [11] R. Latarjet, R. Cramer, and L. Montagnier, "Inactivation, by UV-, X-, and γ -radiations, of the infecting and transforming capacities of polyoma virus," *Virology*, vol. 33, no. 1, pp. 104–111, 1967.
- [12] A. J. Van der Eb and J. A. Cohen, "The effect of UV-irradiation on the plaque-forming ability of single- and double-stranded polyoma virus DNA," *Biochem. Biophys. Res. Commun.*, vol. 28, no. 2, pp. 284–288, 1967.
- [13] H. Werbin, R. C. Valentine, and A. D. McLaren, "PHOTOBIOLOGY OF RNA BACTERIOPHAGES—I. ULTRAVIOLET INACTIVATION AND PHOTOREACTIVATION STUDIES," *Photochem. Photobiol.*, vol. 6, no. 3, pp. 205–213, 1967.
- [14] Z. Zavadova, L. Gresland, and M. Rosenbergova, "Inactivation of single- and double-stranded ribonucleic acid of encephalomyocarditis virus by ultraviolet light.," *Inst. of Virology, Bratislava*, 1968.
- [15] W. Ireland and R. Sacher, "The angular distribution of solar ultraviolet, visible and near-infrared radiation from cloudless skies," *Photochem. Photobiol.*, vol. 63, no. 4, pp. 483–486, 1996.
- [16] "Index of uvradiation_archives_v2."
- [17] V. M. Corman et al., "Rooting the Phylogenetic Tree of Middle East Respiratory Syndrome Coronavirus by Characterization of a Conspecific Virus from an African Bat," *J. Virol.*, vol. 88, no. 19, pp. 11297–11303, 2014, doi: 10.1128/jvi.01498-14.
- [18] A. E. Gorbalenya et al., "The species Severe acute respiratory syndrome-related coronavirus: classifying 2019-nCoV and naming it SARS-CoV-2," *Nat. Microbiol.*, vol. 5, no. 4, pp. 536–544, 2020, doi: 10.1038/s41564-020-0695-z.
- [19] B. W. Neuman et al., "Supramolecular architecture of severe acute respiratory syndrome coronavirus revealed by electron cryomicroscopy," *J. Virol.*, vol. 80, no. 16, pp. 7918–7928, 2006.
- [20] A. R. Fehr and S. Perlman, "Coronaviruses: an overview of their replication and pathogenesis," in *Coronaviruses*, Springer, 2015, pp. 1–23.
- [21] X.-Y. Ge et al., "Isolation and characterization of a bat SARS-like coronavirus that uses the ACE2 receptor," *Nature*, vol. 503, no. 7477, pp. 535–538, 2013.
- [22] N. Zhu et al., "A novel coronavirus from patients with pneumonia in China, 2019," *N. Engl. J. Med.*, vol. 382, no. 8, pp. 727–733, 2020, doi: 10.1056/NEJMoa2001017.
- [23] H. J. Maier, E. Bickerton, and P. Britton, "Coronaviruses: Methods and protocols," *Coronaviruses Methods Protoc.*, vol. 1282, no. 1, pp. 1–282, 2015, doi: 10.1007/978-1-4939-2438-7.
- [24] A. E. Gorbalenya, L. Enjuanes, J. Ziebuhr, and E. J. Snijder, "Nidovirales: Evolving the largest RNA virus genome," *Virus Res.*, vol. 117, no. 1, pp. 17–37, 2006, doi: 10.1016/j.virusres.2006.01.017.
- [25] P. T. Nga et al., "Discovery of the first insect nidovirus, a missing evolutionary link in the emergence of the largest rna virus genomes," *PLoS Pathog.*, vol. 7, no. 9, 2011, doi: 10.1371/journal.ppat.1002215.
- [26] C. M. Walker and G. Ko, "Effect of ultraviolet germicidal irradiation on viral aerosols," *Environ. Sci. Technol.*, vol. 41, no. 15, pp. 5460–5465, 2007, doi: 10.1021/es070056u.
- [27] C. D. Lytle and J.-L. Sagripanti, "Predicted

- Inactivation of Viruses of Relevance to Biodefense by Solar Radiation,” *J. Virol.*, vol. 79, no. 22, pp. 14244 LP – 14252, Nov. 2005, doi: 10.1128/JVI.79.22.14244-14252.2005.
- [28] W. J. Kowalski, “SARS Coronavirus UV Susceptibility,” *Aerobiol. Eng. Rep.*, no. November, pp. 25–28, 2015, doi: 10.13140/RG.2.1.4332.1680.
- [29] M. E. R. Darnell, K. Subbarao, S. M. Feinstone, and D. R. Taylor, “Inactivation of the coronavirus that induces severe acute respiratory syndrome, SARS-CoV,” *J. Virol. Methods*, vol. 121, no. 1, pp. 85–91, 2004, doi: 10.1016/j.jviromet.2004.06.006.
- [30] W. Harm, *Biological effects of ultraviolet radiation*. Cambridge University Press, 1980.
- [31] S. E. Beck, R. A. Rodriguez, M. A. Hawkins, T. M. Hargy, T. C. Larason, and K. G. Linden, “Comparison of UV-induced inactivation and RNA damage in MS2 phage across the germicidal UV spectrum,” *Appl. Environ. Microbiol.*, vol. 82, no. 5, pp. 1468–1474, 2016, doi: 10.1128/AEM.02773-15.
- [32] W. Kowalski, *Ultraviolet Germicidal Irradiation*, vol. 53, no. 9. 2009.
- [33] E. W. Chick, A. B. Hudnell Jr, and D. G. Sharp, “Ultraviolet sensitivity of fungi associated with mycotic keratitis and other mycoses,” *Sabouraudia*, vol. 2, no. 4, pp. 195–200, 1963.
- [34] C. W. Hiatt, “Kinetics of the inactivation of viruses,” *Bacteriol. Rev.*, vol. 28, no. 2, p. 150, 1964.
- [35] E. S. P. B. V, “Veterinary Microbiology, 11 (1986) 41–49,” vol. 11, pp. 41–49, 1986.
- [36] S. M. Duan *et al.*, “Stability of SARS Coronavirus in Human Specimens and Environment and Its Sensitivity to Heating and UV Irradiation,” *Biomed. Environ. Sci.*, vol. 16, no. 3, pp. 246–255, 2003.
- [37] H. Kariwa, N. Fujii, and I. Takashima, “Inactivation of SARS coronavirus by means of povidone-iodine, physical conditions and chemical reagents,” *Dermatology*, vol. 212, no. SUPPL. 1, pp. 119–123, 2006, doi: 10.1159/000089211.
- [38] M. Saknimit, I. Inatsuki, Y. Sugiyama, and K. Yagami, “Virucidal efficacy of physico-chemical treatments against coronaviruses and parvoviruses of laboratory animals,” *Jikken Dobutsu.*, vol. 37, no. 3, pp. 341–345, 1988, doi: 10.1538/expanim1978.37.3_341.
- [39] Y. Liu, Y. Cai, and X. Zhang, “Induction of Caspase-Dependent Apoptosis in Cultured Rat Oligodendrocytes by Murine Coronavirus Is Mediated during Cell Entry and Does Not Require Virus Replication,” *J. Virol.*, vol. 77, no. 22, pp. 11952–11963, 2003, doi: 10.1128/jvi.77.22.11952-11963.2003.
- [40] M. Eickmann *et al.*, “Inactivation of Ebola virus and Middle East respiratory syndrome coronavirus in platelet concentrates and plasma by ultraviolet C light and methylene blue plus visible light, respectively,” *Transfusion*, vol. 58, no. 9, pp. 2202–2207, 2018, doi: 10.1111/trf.14652.
- [41] M. Eickmann *et al.*, “Inactivation of three emerging viruses – severe acute respiratory syndrome coronavirus, Crimean–Congo haemorrhagic fever virus and Nipah virus – in platelet concentrates by ultraviolet C light and in plasma by methylene blue plus visible light,” *Vox Sang.*, vol. 115, no. 3, pp. 146–151, 2020, doi: 10.1111/vox.12888.
- [42] R. Lu *et al.*, “Genomic characterisation and epidemiology of 2019 novel coronavirus: implications for virus origins and receptor binding,” *Lancet*, vol. 395, no. 10224, pp. 565–574, 2020, doi: 10.1016/S0140-6736(20)30251-8.
- [43] P. Zhou *et al.*, “A pneumonia outbreak associated with a new coronavirus of probable bat origin,” *Nature*, vol. 579, no. 7798, pp. 270–273, 2020, doi: 10.1038/s41586-020-2012-7.
- [44] R. Sah *et al.*, “Complete genome sequence of a 2019 novel coronavirus (SARS-CoV-2) strain isolated in Nepal. Microbiol. Resour. Announc. 9, e00169-20.” 2020.
- [45] F. Wu *et al.*, “A new coronavirus associated with human respiratory disease in China,” *Nature*, vol. 579, no. 7798, pp. 265–269, 2020, doi: 10.1038/s41586-020-2008-3.
- [46] J. Herman, B. Biegel, and L. Huang, “Inactivation times from 290 to 315 nm UVB in sunlight for SARS coronaviruses CoV and CoV-2 using OMI satellite data for the sunlit Earth,” *Air Qual. Atmos. Heal.*, pp. 1–17, 2020.
- [47] J. Sagripanti and C. D. Lytle, “Estimated Inactivation of Coronaviruses by Solar Radiation With Special Reference to COVID-19,” *Photochem. Photobiol.*, 2020.

الخلاصة

تعتبر الأشعة فوق البنفسجية الشمسية المنبعثة من الشمس المصدر الرئيسي لآبادة الجراثيم والتعقيم البيئي. الهدف من هذه الدراسة هو تقدير مقدار جرعة الأشعة فوق البنفسجية والوقت اللازمين لتعطيل فيروسات كورونا بالتعرض للشمس. تم فحص وتلخيص التجارب المنشورة على جرعة 254 نانومتر لتعطيل الأشعة فوق البنفسجية عند التعرض للأشعة فوق البنفسجية لعائلات فيروسات كورونا والميكروبات المكافئة من حيث D90 (جرعة الأشعة فوق البنفسجية لتثبيط 90%) ، أو أي جرعة أخرى و / أو حجم الجينوم. تم افتراض المتوسط مع مجال الثقة الزمني لجرعة تعطيل D90-254 نانومتر الموحدة لجميع التجارب على أنها قابلية للأشعة فوق البنفسجية لفيروس SARS-CoV-2 (COVID-19) تم اعتماد طيف جرعة التعطيل (مغلف الحساسية) لفيروسات كورونا والميكروبات المكافئة كدالة لطول موجة الأشعة فوق البنفسجية المكافئ لنطاق الأشعة فوق البنفسجية (280 إلى 320 نانومتر) من الأدبيات. تم استخدام كثافة القياس الشمسي للأشعة فوق البنفسجية في الموقع الجغرافي لبغداد على مدار عام في كل خمسة عشر دقيقة وتم تحويلها من مجموع قطوع إلى طيف شمسي لكل طول موجي في نطاق 280 إلى 320 نانومتر باستخدام نموذج رياضي مبسط. تم رسم طيف عمل مركب يتضمن طيف حساسية الفيروس الذي تم تسويته إلى 254 نانومتر ، طيف قياسات الأشعة فوق البنفسجية الشمسية ، وتعطيل طيف الجرعة الفعالة لفيروسات كورونا. تم حساب المنطقة الواقعة تحت طيف الجرعة الفعالة للتثبيط عددياً للعثور على التدفق الشمسي المكافئ. يتم توقع الوقت اللازم لتعطيل فيروس SARS-CoV-2 (COVID-19) لكل قيمة من شدة مجموع الأشعة فوق البنفسجية لمحاكاة الوقت المطلوب لتعقيم الأسطح الخارجية في جميع الأشهر مع موقع بغداد الجغرافي. يجب أن يكون هذا العمل مفيداً لتزويد صانعي القرار بصورة واضحة عن إدارة عملية التعقيم للأسطح الخارجية وترتيب توقيت حظر التجول